A Time Dependent Model for CdTe PV Module Temperature in Utility Scale Systems

William Hayes, Lauren Ngan

First Solar, San Francisco, CA, 94105, USA

***Abstract* — A model for PV module temperature is developed and validated for fixed tilt utility scale PV systems. The solution proposed allows for the modeling of PV module temperature at time scales less than one hour by introducing a time dependency of the module temperature based on module heat capacity. The model is found to be more accurate than commonly used PV module temperature models at both the hourly and sub-hourly time scales. Results suggest an increase in modeling accuracy based on the energy weighted mean absolute error by a minimum of 0.2 °C to a maximum of 2.0 °C.**

***Index Terms* —performance modeling, solar photovoltaics, temperature, CdTe**

I. Introduction

The temperature of PV modules has the second largest impact on the energy generation of PV systems, second only to the amount of incident irradiance on the PV modules. An accurate representation of module temperature is critical to the overall accuracy of a PV system performance model. Most commercially available PV system modeling software, including PVsyst, implements steady-state module temperature models that operate on hourly averaged data [1]. These models assume proportionality between incident irradiance and module temperature with ambient temperature and wind speed having affects as well. It has been proven that such models can be optimized but there are limitations to their accuracy which results in inaccuracies in modeling PV system energy generation [2]. This is due to the simplicity of the functional form of the model as well as the hourly averaged time scale, which has its detriments, as noted by [3], [4], and [5].

These modeling deficits highlight a need to develop better capabilities with regards to module temperature modeling in order to provide a higher level of accuracy in PV system energy predictions. To achieve this goal, a model is developed following the same methodology as [6] and [7] which use the heat balance equation. This is a time dependent model ("TD") that introduces additional modes of heat transfer and heat storage to the solution for module temperature. The model is applied to seven different utility scale PV systems that have a minimum of one year of operation and are located in two distinctly different climatic regions (hot/desert and temperate). This dataset covers a span of 11 years of system operation as detailed in Table I.

II. Model Development

Module cell temperature will be governed by the heat balance equation. Previous models have relied on hourly averaged data as input which has motivated model developers to assume the system is at steady state greatly simplifying the module temperature model. In contrast, this model is developed such that it can be applied to a broader range of modeling intervals including hourly and sub-hourly time steps.

By applying the heat balance equation to a PV module we arrive at (1). In this equation conductive heat transfer between the module and the mounting system is assumed to be negligible due to the use of thick rubber clamps which serve as a layer of insulation from heat transfer.

$$C_{module}\frac{dT_{module}}{dt} = \dot{q_{lw}} + \dot{q_{sw}} + \dot{q_{conv}} - \dot{P_{out}} \quad (1)$$

The remaining terms in (1) refer to radiation (long and short wave), convection, and electrical power. Manipulating (1) provides a solution for the module temperature at a specific timestep, $t = t+dt$, given the conditions at the previous time step, $t = t$, and the associated heat balance terms.

$$T_{t+dt} = \frac{dt}{C_{mod}}\left(\dot{q_{lw}} + \dot{q_{sw}} + \dot{q_{conv}} - \dot{P_{out}}\right) + T_t \quad (2)$$

A. Radiative Heat Transfer

Radiative heat transfer is divided into long wave radiation (q_{lw}) and short wave radiation (q_{sw}). Short wave radiation originates from the sun and includes direct beam irradiance and diffuse irradiance. The amount of short wave radiation that reaches the PV cell will be equal to the plane of array irradiance accounting for optical losses on the front side of the PV modules. This parameter is referred to as the effective plane of array irradiance, POA_{eff}, as in (3).

$$\dot{q_{sw}} = POA_{eff} \quad (3)$$

Long wave radiation consists of the radiative interactions between the module and objects within the Earth's atmosphere. This includes the ground, the sky, and nearby PV modules as noted in (4).

$$\dot{q_{lw}} = \dot{q_{mod\leftrightarrow sky}} + \dot{q_{mod\leftrightarrow ground}} + \dot{q_{mod\leftrightarrow mod}} \quad (4)$$

TABLE I
SUMMARY OF MODELING ASSUMPTIONS

System No.	Köppen-Geiger Climate Classification	Simplified Climate Classification	System Reference Name	Date Range
1	BWh (Arid Desert Hot)	Hot	H1, H2, H3	1/1/2010 - 12/31/2012
2	BWh	Hot	H4	1/1/2012 - 12/31/2012
3	BWh	Hot	H5	1/1/2012 - 12/31/2012
4	BSk (Arid Steppe Cold)	Hot	H6, H7	1/1/2011 - 12/31/2012
5	Dfb (Snow, Fully humid; Warm summer)	Temperate	T1, T2	1/1/2011 - 12/31/2012
6	Dfb	Temperate	T3	1/1/2012 - 12/31/2012
7	Dfb	Temperate	T4	1/1/2012 - 12/31/2012

Each term in (4) is defined as:

$$\dot{q_{1\leftrightarrow 2}} = \sigma A(\varepsilon_1 VF_{1\to 2}T_1^4 - \varepsilon_2 VF_{1\to 2}T_2^4) \quad (5)$$

where:

σ : Stefan-Boltzmann constant
A : Module Area
ε : Emissivity
VF : View Factor
T : Temperature (K)

The view factor represents the percentage of the hemispherical dome viewed from object one (the PV module) that is occupied by object two. For this case, the reference point on the module is assumed to be at the midpoint of the module row height. As radiation is emitted from both the front and the back of the modules, the summed total of view factors will be two. It is assumed that the module row length is sufficiently large enough such that the view factor is consistent across all PV modules and the three dimensional hemisphere can be approximated by the two dimensional arc that is in normal to the plane of the module.

B. Convective Heat Transfer

Convection is the most dynamic contribution to the overall heat balance equation and is defined in (6):

$$\dot{q_{conv}} = (k_c + k_v * WS_{2.5m})(T_{module} - T_{air}) \quad (6)$$

The terms k_c and k_v represent the free and forced convection terms, respectively. The wind speed value, $WS_{2.5m}$, is measured at a height of 2.5 meters. This height has been chosen based on the height of wind speed measurements that were available for operational First Solar PV power plants. This data was used for model development and serves as the most accurate reference point for this model. When values for wind speed are not available at this height, the value can be extrapolated to 2.5 meters from a height, X, using the log wind profile described by (7) [8].

$$WS_{2.5m} = WS_X \frac{\ln\left(2.5/z_0\right)}{\ln\left(X/z_0\right)} \quad (7)$$

The term z_0 refers to the aerodynamic roughness length and is determined by the surrounding landscape. The majority of utility scale PV systems are installed in open areas where obstacles have been introduced to the flow field. Such obstacles, including inverter shelters and PV modules, motivate a selection of roughness length of z_0 = 0.25 m per the Davenport-Wieringa roughness length classification. It is expected that the roughness length for a specific site will vary around this theoretical value and can introduce error into the model (Fig. 1). Assuming a range of site specific roughness lengths that spans 0.15 m ≥ z_0 ≥ 0.35m would introduce errors in $WS_{2.5m}$ of roughly ± 7%. The magnitude of this uncertainty is addressed in sensitivity analysis presented in the following section.

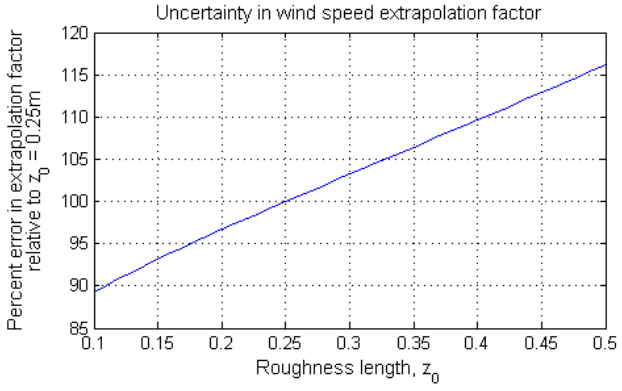

Fig. 1. Uncertainty in the wind speed extrapolation factor relative to an assumed roughness length of z_0 = 0.25 meters.

C. Electrical Energy

A portion of the incoming solar irradiance is converted into electrical energy which is drawn from the PV modules through the cabling. This energy is not converted into thermal heat and therefore must be removed from the heat balance equation. This is described by (8):

$$\dot{P_{out}} = Eff_{mod} * POA_{eff} * A \quad (8)$$

Where Eff_{mod} is the module efficiency and POA_{eff} and A are effective POA and module area as previously noted.

III. Sensitivity Analysis

Measurement points for all parameters in (4), (5), and (6) are not available. The unknown parameters include C_{mod}, ε_{gnd}, ε_{sky} T_{gnd}, T_{sky}, k_c, and k_v. To address the sensitivity associated with each parameter, a series of analyses were undertaken on one-minute resolution data to evaluate the accuracy of expressing each term either as a constant or as an expression that relies on a measurement point. Efforts to resolve the sensitivity of these parameters using annual datasets required upwards of 100 hours of computational time per site using the hardware available. These constraints motivated the use of monthly datasets spanning all seasons and a subset of locations to capture seasonal and climate effects.

Initial assumptions were generated for the unknown terms based on available measurements and documented physical properties. It was assumed that the temperature of the ground could be represented by the module temperature with a static offset. Likewise, the sky temperature was assumed to be the same as the ambient air temperature with a static offset.

Rather than attempt to solve a seven dimensional space to minimize model error, an iterative approach to evaluating the model's sensitivity to each parameter was executed. Default values based on initial assumptions were assigned to each parameter and iterated upon in sequence to determine the relative sensitivity of the model to an individual parameter using the irradiance weighted mean absolute error. From this analysis it was determined that the model is primarily sensitive to the convective heat coefficients, k_c and k_v. See Fig. 2-4. It is also observed that sensitivity of the model to the range of uncertainty introduced by the extrapolation of wind speed (± 7%) falls within the error trough shown in Fig. 4. The resulting distribution of weighted mean absolute error that is generated by the extrapolation uncertainty is within 0.2 C which is deemed acceptable given the limitations of measurement accuracy.

Although not pictured, it was also determined that the model is insensitive to the module heat capacity over the range of reasonable values spanning 800 to 1100 J/kg·K. Therefore, the heat capacity for glass of 840 J/ kg·K is used without the inclusion of heat capacity of the solar cells.

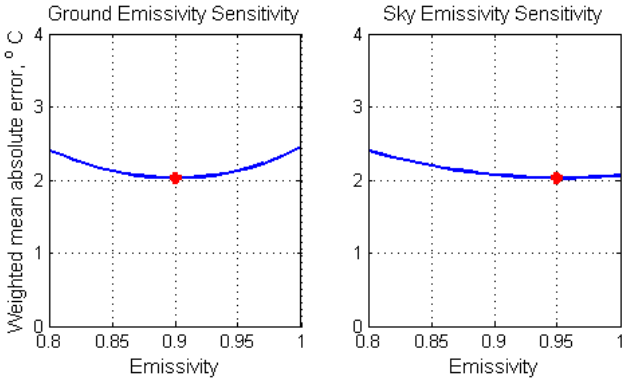

Fig. 2. Sensitivity of irradiance weighted mean absolute error to emissivity parameters with default assumptions noted by red asterisk.

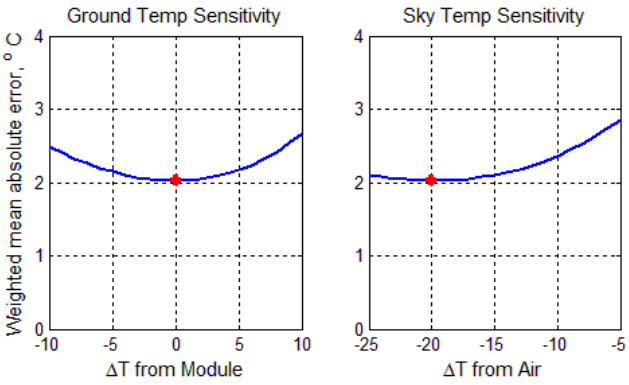

Fig. 3. Sensitivity of irradiance weighted mean absolute error to temperature parameters with default assumptions noted by red asterisk.

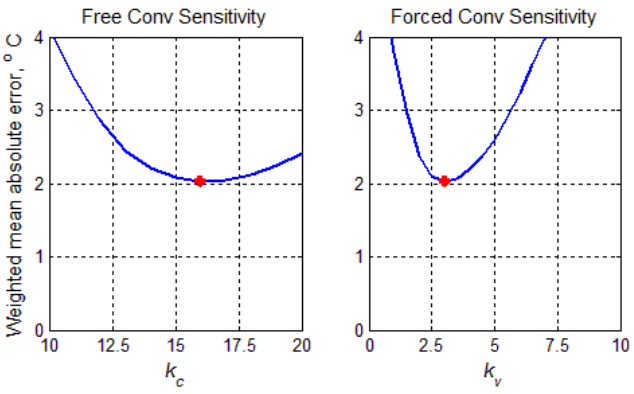

Fig. 4. Sensitivity of irradiance weighted mean absolute error to convective heat transfer coefficients with default assumptions noted by red asterisk.

IV. Error Minimization

Understanding gleaned from the sensitivity analysis was leveraged to simplify the error minimization effort. This includes error minimization efforts focused on the convective loss coefficients as well as the error associated with the time scale that is used for model execution.

A. Convective Loss Coefficients

Iterating upon the secondary sensitivity parameters over a narrow range of convective coefficient pairs highlighted a commonality in these parameters that reduced error for each of the monthly one-minute datasets. Therefore the values of the secondary parameters were set as noted in Table II and attention was then focused on determining the convective heat loss coefficients that minimized error.

TABLE II
SUMMARY OF MODELING ASSUMPTIONS

Variable	Assumption
T_{sky}	$T_{ambient}$ – 20 °C
T_{ground}	T_{module}
ε_{sky}	0.95
ε_{ground}	0.85 / 0.9 (sand / grass)
C_{mod}	840 J/kg*K

Attempting to minimize the annual error in the 11 year dataset highlighted a trend that suggests that different (k_c, k_v) pairs are more accurate for different climate types. The contour plots in Fig. 5 highlight these differences as the error minimization trough differs between a representative hot climate and a representative temperate climate.

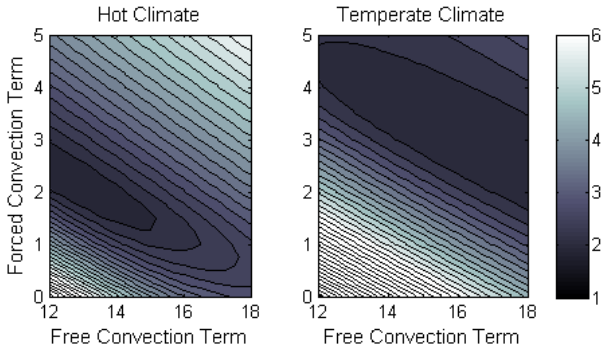

Fig. 5. Weighted mean absolute error contour plot for a hot climate (left) and temperate climate (right).

The distinct difference in the convective coefficient pairs that minimize error is believed to be driven by differences in latent heat flux driven by evapotranspiration could be causing this difference. This requires a bifurcation in the convective coefficients of the thermal model in order to increase the accuracy. The convective coefficients for hot and temperate climates which minimize model error are as shown in Table III.

TABLE III
CONVECTIVE COEFFICIENT DEFINITIONS

Climate	(k_c, k_v)
Hot	*(12.7, 2.0)*
Temperate	*(16.5, 3.2)*

It must be noted that the climate classifications of "hot" and "temperate" for this exercise are not consistent in nomenclature with the Köppen-Geiger climate classification. The PV systems defined as "hot climate" in this work are located in Dry (B) and Temperate (C) zones. The PV systems defined as "temperate climate" are located in Cold (D) zones.

B. Modeling Timestep

The modeling parameters previously defined have been determined based on one-minute resolution data which is not always available as a modeling input. Typical PV modeling is restricted to hourly average data, such as in PVsyst. Therefore a review of the accuracy of (2) must be evaluated using different averaging intervals to provide insight into the model's applicability at less granular temporal resolution. Given the computational cost of running annual one-minute datasets as previously noted, a preliminary understanding of the impact of modeling timestamp on accuracy is developed using monthly datasets. This understanding can then be applied to annual datasets to evaluate annual error in the time dependent model. The error associated with the monthly dataset analyzed grows rapidly as the time interval increases (Fig. 6). This is a result of the finite-difference solution to (1) being applied to increasing time intervals that introducing error. More importantly, the weighted mean absolute error for the time dependent model is larger than the simpler model used in PVsyst for time intervals greater than five minutes.

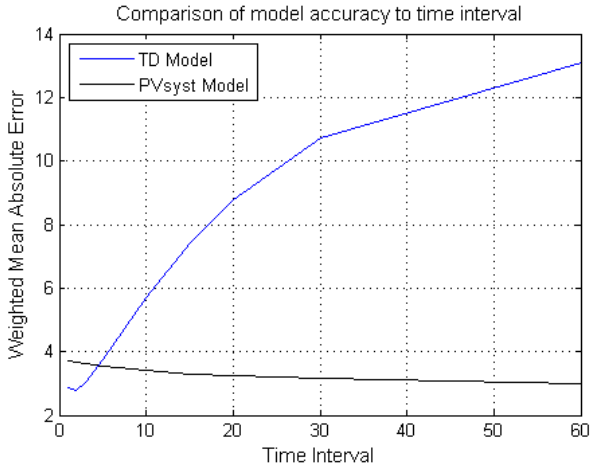

Fig. 6. Weighted mean absolute error for time dependent model (TD) and the PVsyst model at different time intervals.

To address the inaccuracies when modeling data at larger timescales, a linear interpolation can be applied to hourly data to construct a dataset that represents higher temporal resolution data. The time-dependent model run with hourly data with a five-minute interpolation interval produced lower weighted mean absolute error metrics relative to the PVsyst thermal model results for all annual datasets analyzed. See Fig. 7.

V. Model Validation

The model was applied to the annual datasets and the hourly residuals were evaluated. This allows for a direct comparison in model accuracy between (2) and conventional thermal models being applied in industry, such as in PVsyst. For each dataset, the cell temperature of the module was determined per King [9] which accounts for the difference between cell temperature and the measured temperature at the back of the PV module. For each system analyzed, a decrease in the irradiance weighted mean absolute error was observed with the time-dependent model. This range spans 0.2 to 2 degrees Celsius which translates to 0.05% to 0.4% impact on annual energy generation for a temperature coefficient of 0.29% per degree Celsius.

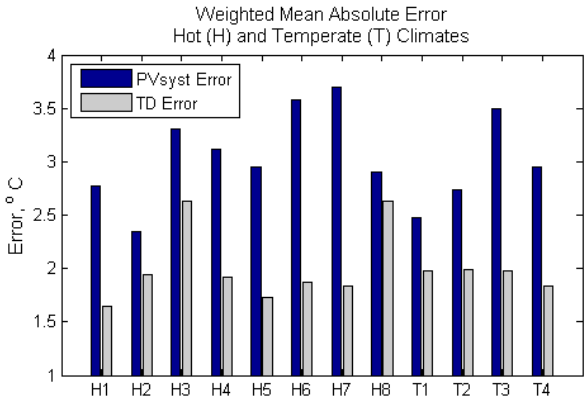

Fig. 7. Change in annual weighted mean absolute error between PVsyst thermal model and time dependent (TD) model.

Further support of the accuracy of the time dependent model relative to the PVsyst thermal model can be observed in Fig. 8. The plots represent comparisons of the hourly averaged measured module temperature to hourly modeled module temperature for both the time dependent model and the model used in PVsyst. It is apparent that the time dependent model is able to more accurately characterize the module temperature, particularly at low irradiance. In addition, a drastic decrease in the root mean square error is observed for the time dependent model.

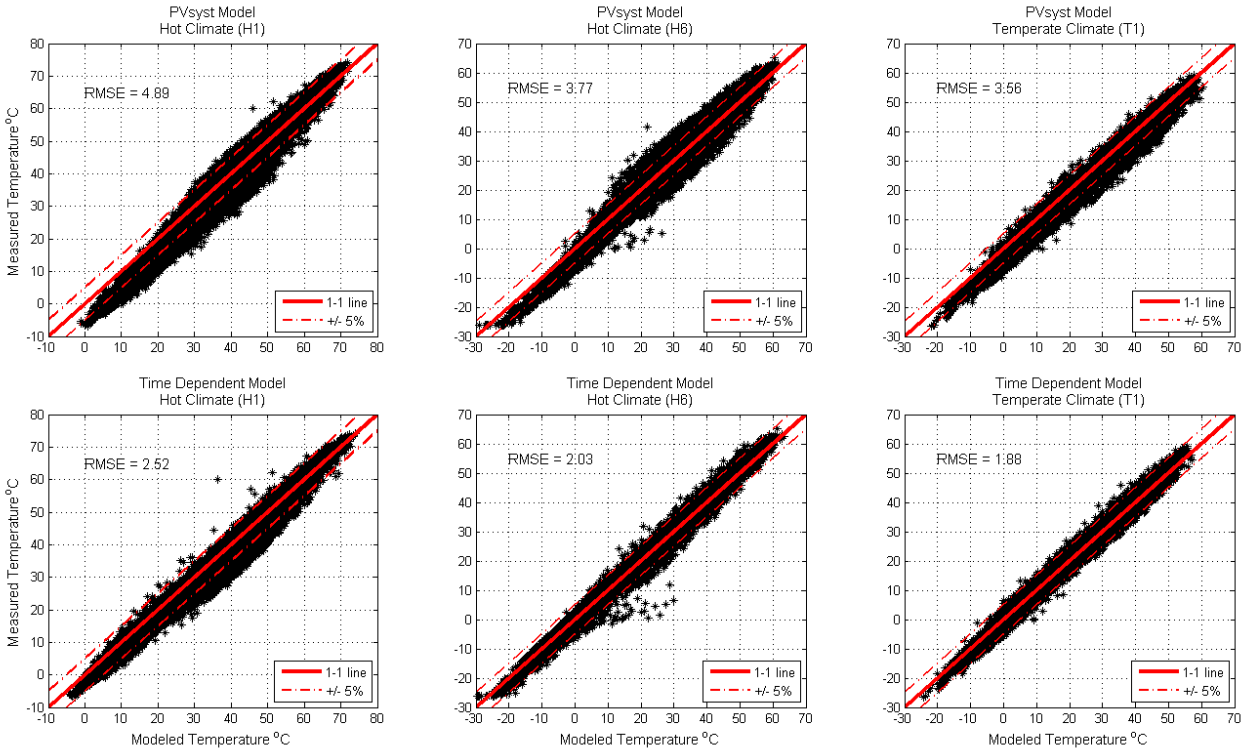

Fig. 8. Plots of hourly measured versus modeled module temperature for three PV systems. Top: PVsyst thermal model with one-hour modeling timestep; Bottom: Time Dependent model with one-hour modeling timestep with five-minute interpolation interval.

VI. Conclusion

A time dependent model for evaluating the module temperature of Cadmium Telluride PV modules in fixed tilt utility-scale systems is developed and validated. The model is applicable at sub-hourly time intervals to better characterize the dynamics of module temperature. The time dependent model can also be applied to hourly averaged data using a five-minute interpolation time step to achieve a more accurate solution than commercially available PV simulation software. The increase in modeling accuracy for the 11 years of system operation that were analyzed spans the range of 0.2°C to 2.0-°C.

References

[1] "PVSYST: Photovoltaic Software." Retrieved February 10, 2014 from http://www.pvsyst.com.

[2] W. Hayes, L. Nelson, and A. Panchula, "Thermal Model Accuracy of Hourly Averaged Data for Large Free Field Cadmium Telluride PV Arrays." *Proc. IEEE PVSC 38*, Austin, TX, USA, 2012.

[3] C. Hansen, J. Stein, and D. Riley, "Effect of Time Scale Analysis of PV System Performance." Sandia National Laboratory, Albuquerque, NM, SAND2012-1099. Feb. 2012.

[4] S. Ransome and P. Funtan. "Why Hourly Averaged Measurement Data is Insufficient to Model PV System Performance Accurately." *Proc. 20th European PVSEC* Barcelona, Spain 2005.

[5] W. Hayes, L. Nelson, and M. Francis, "Improving Hourly PV Power Plant Performance Analysis: Irradiance Correction Methodology." *Proc. IEEE PVSC 39*, Tampa Bay, FL, USA, 2013.

[6] A. Luketa-Hanlin and J. Stein, "Improvement and Validation of a Transient Model to Predict Photovoltaic Module Temperature." *World Renewable Energy Forum*, Denver, CO, USA 2012.

[7] A.D. Jones and C.P. Underwood, "A Thermal Model for Photovoltaic Systems." *Solar Energy*, vol. 70, No. 4, pp. 349-359 2001.

[8] R. B. Stull, "*Meteorology for Scientists and Engineers.* Pacific Grove, California: Brooks/Cole 2000.

[9] D. King, W. Boyson, and J. Kratochvil., "Photovoltaic Array Performance Model." Sandia National Laboratory, Albuquerque, NM, SAND2004-3535. Aug. 2004.